JOURNAL OF CATALYSIS 113, 129–143 (1988)

Sintering of Silica-Supported Platinum Catalysts during Ethylene Oxidation

N. L. WU AND J. PHILLIPS[1]

Department of Chemical Engineering, The Pennsylvania State University, 133 Fenske Laboratory, University Park, Pennsylvania 16802

Received August 6, 1987; revised December 10, 1987

X-ray diffraction was used to determine the changes in particle size distribution of silica-supported platinum particles following treatments in reactive ($C_2H_4 + O_2$) and nonreactive control (O_2, CO_2, H_2O, C_2H_4) atmospheres for varying lengths of time at 600°C. The nature of the observed changes for reactive atmosphere-treated samples was very different from that for control atmosphere-treated samples. Modeling work indicated that the changes in the particle size distribution found following treatment in any nonreactive atmosphere were consistent with particle growth by coalescence, whereas under reaction conditions changes in the particle size distribution were consistent with growth by atomic migration. It is suggested that under reaction conditions the sintering process is dominated by the formation of volatile, metastable platinum containing intermediates which form via the interaction of homogeneously formed radicals with supported platinum particles.

INTRODUCTION

Supported metal catalysts show changes in total metal surface area after high-temperature heating and following their use in catalytic processes. These treatments generally result in a decrease in the total metal surface area due to the growth of metal particles, a process known as sintering. Previous studies in this area, conducted in single gas atmospheres such as in a vacuum oxygen, and hydrogen, indicate that, in addition to temperature, sintering of metal catalyst is rather sensitive to the chemistry of the gas atmosphere (*1–5*). More significantly, several studies on the surface reconstructions, or catalytic etching (*6*), of metal foils (*6, 7*) and thin films (*8*) in reactive atmospheres have clearly shown that unprecedented massive metal migration can take place under certain reaction conditions resulting in significant changes in both foil surfaces and thin film structures. It was also demonstrated that this type of structural change was definitely not the sum of the etching effects due to each single reactant and reaction product species. These results suggest that it is reasonable to presume that the sintering phenomenon taking place under reaction conditions is qualitatively different from that taking place in a single gas or under vacuum. Thus, a study of sintering of supported catalysts under reaction conditions is warranted.

The present work is a report on the sintering studies of silica-supported platinum catalysts which takes place during ethylene oxidation. One of the major objectives of this study was to determine how the enhanced platinum migration, observed in previous etching studies, can affect the sintering of platinum catalysts under similar conditions. This work represents an effort to build a bridge between the catalytic etching studies and the sintering studies of metal catalysts. In brief, it was found by using X-ray diffraction (XRD) that sintering of silica-supported platinum catalysts under ethylene oxidation at 600°C followed the interparticulate atomic transport mechanism, with almost no coalescence growth at all, while in oxygen, ethylene, carbon diox-

[1] To whom correspondence should be addressed.

0021-9517/88 $3.00

ide, and water-containing atmospheres, in which no reaction process was taking place, platinum particles grew primarily via the coalescence mechanism. Apparently under the reaction conditions there was an increase in the platinum transport in atomic form and a reduction in platinum particle movement. The increase in the platinum atomic migration under these conditions is consistent with the results seen in previous etching studies. Furthermore, the decrease in the mobility of platinum particles found under the reaction conditions may be due to adsorbed H_2O and/or, particularly under C_2H_4-excess conditions, carbon deposited on the surface during the reaction. That is, the control studies indicated that the particle motion is reduced during treatments in $H_2O/O_2/N_2$ (2/6/92) and in C_2H_4/N_2 (2/98) treatments relative to that in dry O_2 atmosphere.

In all atmospheres there was found to be an initial period during which the large particles in the distribution grew smaller. The behavior of the smaller particles is dominated by coalescence growth from the beginning. This initial decrease in the size of the large particles is shown to be consistent with earlier studies and is attributed to the cracking and/or spreading of unstable particles, as described by other workers.

EXPERIMENTAL

The supported platinum catalysts used in this study were prepared as follows: $Pt(NH_3)_4(NO_2)_2$ dissolved in water was mixed with silica gel (Grade 57, Davison), and the final solution dried in air at 100°C for 16 h. The final Pt loading was about 2%. All catalyst samples (approximately 1 g each) were then further presintered, in batches, under vacuum at 200°C for 1 h and in oxygen at 500°C for another 0.5 h. The final step was to ensure that all the platinum precursors were decomposed to leave pure platinum crystallites (*9*). During the sintering experiments, each sample was repeatedly used in the same atmosphere in order to follow the sintering phenomena, i.e., the changes in its particle size distribution.

The reactor system used in this study consisted of a tubular quartz reactor, a high-temperature oven, and a conventional glass high-vacuum, gas-handling system. The quartz reactor consisted of a preheating section and a reaction cell. A side arm connected directly to the reaction cell was attached for easy sample loading and unloading. During the heat treatments, platinum catalysts were loaded inside the cell similar to a simple fixed bed operation. A thermocouple well was located at the center of the cell to facilitate sample temperature reading and furnace control. The reaction temperature throughout this study was set at 600°C, which is within the temperature range where enhanced Pt transport during ethylene oxidation was observed in previous etching studies (*7, 8*). In the studies of sintering under reaction conditions both fuel excess and oxygen excess conditions were employed. It has been shown in previous work with both thin films and platinum foils (*7, 8*) that under fuel excess conditions reaction-induced surface temperature gradients will be small, and under oxygen excess conditions the gradients can be quite large. In the present study the difference in temperature between the oven temperature and the average catalyst bed temperature (always 600°C) never exceeded 1°C. Thus, there was no indication that temperature gradients were great under any conditions.

X-ray diffraction was used to determine both the average particle size and the particle size distributions of platinum crystallites. The latter were calculated based on the Fourier analysis (*10, 11*) of the Pt(111) X-ray line profile acquired from each sample. This method has been extensively tested and employed in the field of metallurgy over the last 30 years (*12*) and is becoming one of the standard methods for determining the particle size distribution for supported catalysts. The theory has been developed and discussed elsewhere (*13–15*). It has been found in earlier studies that the size of supported particles less than 20 Å can be determined unambiguously

using this method (*16–19*). In addition, multimodal distributed PSDs have frequently been observed using this method (*9, 10, 18*).

Some earlier workers (*13, 14, 18*) found it necessary to smooth the raw X-ray data. In the present study instead of smoothing the raw data, the following procedure was employed. The Fourier coefficients, obtained directly from the raw X-ray data, were smoothed using the cubic spline method. The smoothed coefficients were then used to produce X-ray spectra, which were carefully compared to the raw X-ray spectra to make certain no artificial features had been introduced due to the smoothing procedure. It was found in all cases that the smoothed spectra faithfully reproduced the raw spectra, minus the high-frequency "noise" found in some cases far from the peak center (see Fig. 1).

The instrumental broadening profile was acquired from a platinum foil sample which had been annealed under vacuum for 48 h at 1000°C. These data were needed to calculate the pure X-ray line profile, i.e., the line profile without the instrumental broadening effect, using the method of Stokes (*14*). The strain coefficient was calculated using the single peak method developed by earlier workers (*15, 16*).

The X-ray diffractometer (Rigaku DMAX-IA) used in the present study employs a copper target X-ray source, curved crystal monochrometer, and Tl-drifted NaI scintillation detectors. In this study the X-ray data were collected at a scanning rate of one-quarter degree per minute, and the step size used was 0.0125°. The baseline correction was obtained from the spectra of unimpregnated SiO_2 powders of the same type used to make the samples. In other words, a blank silica sample was prepared for each condition. These powders were subjected to heat treatments similar to that given to the samples reported on in this study.

The total support (SiO_2) surface area was measured using the BET method (N_2) before and after the heat treatments. It was found that the support surface area was insensitive to the treatments encountered in this study and remained in the range 210 ± 10 m^2/g following all treatments, close to that reported by the manufacturer (220 m^2/g).

RESULTS

Most earlier sintering studies have used the changes in the "average particle size" obtained from different methods to characterize the observed sintering process. However, as described later, it was found that the platinum samples used in this study consisted of a very broad particle size distribution (PSD) and that the "average particle size" calculated from different methods varies significantly. It was found that changes of these average values did not satisfactorily represent the sintering process of the whole sample. Thus, in the following section, the sintering of platinum catalysts will be described based on the changes in the PSDs. In most cases, qualitative changes in the PSDs can be perceived directly from the changes in the shape of X-ray line profiles, without any need for mathematical analysis. The Fourier analysis also gives reliable qualitative information. Thus, the focus of the following section is on the rough "shape" of the particle size distribution and on trends in the changes of this rough shape, rather than absolute numbers.

Sample as prepared. XRD showed that the X-ray line profile of the as-prepared Pt catalysts always consisted of a very broad base with a sharp peak at the reflecting angle (Fig. 1a). Simple least-squares fitting indicated that these reflections were neither Gaussian nor Cauchy types of line profiles as assumed in many earlier XRD studies. In fact, the average particle size (Table 1) calculated from the Debye–Sherrer equation using half-intensity width ($D_{1/2}$) is ~230 Å, which is almost two times larger than that calculated from the integrated breadth (D_I), ~130 Å. For typical Gaussian and Cauchy types of line profiles the difference between these two "average particle sizes" is less

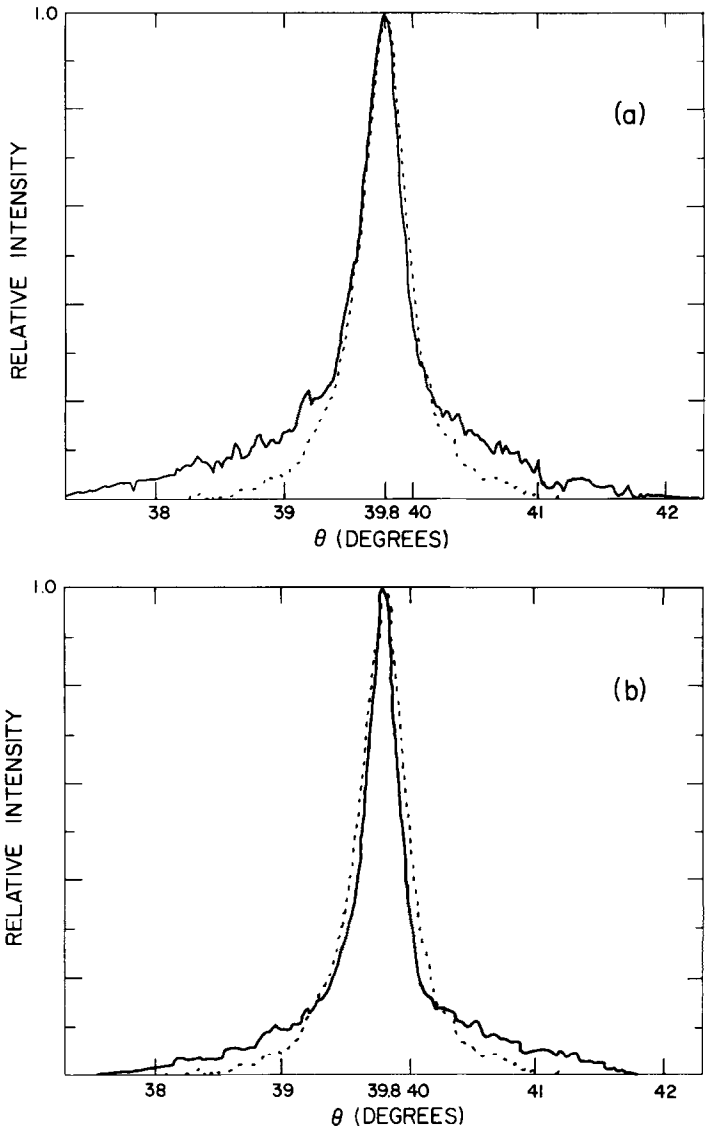

FIG. 1. XRD line profiles from Pt(111) reflections. (a) The solid curve is the XRD line profile, obtained from the sample prior to treatments at 600°C. The dashed curve is the XRD line profile following treatment in O_2/N_2 (8/92) at 600°C for 64 h. (b) The dashed curve is the line profile after O_2/N_2 (8/92) treatment for 64 h at 600°C. The solid curve is the line profile after $C_2H_4/O_2/N_2$ (2/5/93) for 64 h.

than 10% over the particle size range considered (*20*). Indeed, the large difference between these two values indicates a very broad PSD (*21*).

Fourier analysis of the Pt(111) profile gave a PSD (Fig. 2) consisting of a high-intensity small-particle peak at 20 Å and a long large-particle tail extending to the particle size up to 300 Å. It should also be noted that the $D_{1/2}$ (230 Å), calculated from the Debye–Sherrer equation, is heavily weighted toward the large-particle portion of the distribution curve (Fig. 2). In fact, neither D_1 (130 Å) nor $D_{1/2}$ (230 Å) coincides

with any significant features shown in the PSD. Finally, the microstrain calculated assuming a Gaussian type of strain distribution (*10, 22*) is negligible ($(\langle e^2 \rangle (20\ \text{Å}))(\frac{1}{2}) = 0.3 \times 10^{-2}$ where $\langle e^2 \rangle$ is the mean square of the microstrain (*10*)) and has little effect on the PSD. This is consistent with the earlier XRD studies on Pt/SiO_2 catalysts (*21*).

Sintering in nonreactive gas treatment. Studies conducted in nonreactive atmospheres were primarily carried out as control experiments, so that the effect of the individual gases on the sintering process could be clearly determined. A comparison of the results of these control experiments with the results of reactive gas atmosphere studies allows for a clearer understanding of the special effect that reaction conditions have on the sintering process. For this reason the individual gases used in the control studies were mixed with nitrogen as a carrier gas (just as they are under reaction conditions) and their concentrations kept to approximately the same levels as are found under reaction conditions. The gases used in this study were oxygen, carbon dioxide, water, and ethylene as these are the principal reactants and products of ethylene oxidation over platinum.

TABLE 1

Sintering—Sample History and Average Particle Size

Sample no.	History	Average particle size (Å)		
		$D_{1/2}$	D_1	$D_{1/2}/D_1$[b]
0	As prepared	230	130	1.77
0-1	6% O_2/94% N_2, 16 h	190	140	1.36
0-2	6% O_2/94% N_2, 32 h	210	160	1.31
0-3	6% O_2/94% N_2, 64 h	210	170	1.24
0-3[a]	Same as 0-3 + 5% O_2/2% C_2H_4/93% N_2, 20 h	250	180	1.39
0-W	Wetted 6% O_2/94% N_2, 16 h	190	130	1.46
E-1	2% C_2H_4/98% N_2, 16 h	190	120	1.58
II-1	8% O_2/2% C_2H_4/90% N_2, 32 h	210	140	1.50
II-2	8% O_2/2% C_2H_4/90% N_2, 64 h	250	150	1.67
III-1	5% O_2/2% C_2H_4/93% N_2, 16 h	230	120	1.90
III-2	5% O_2/2% C_2H_4/93% N_2, 32 h	270	150	1.80
III-3	5% O_2/2% C_2H_4/93% N_2, 64 h	320	170	1.88

[a] The average particle size is calculated by using Debye–Scherrer equation based on the half-intensity width for $D_{1/2}$ and integrated breadth for D_1, respectively.

[b] The $D_{1/2}/D_1$ ratio shows the departure of XRD line profile from the Gaussian behavior, of which the ratio is less than 1.10.

XRD studies showed that, following prolonged treatments in O_2/N_2 (6/94, see Table 1) at 600°C, the sintered platinum catalysts gave X-ray reflections closer to the Gaussian type of line profiles. That is, while the width at half-maximum intensity of the Pt(111) peak was only slightly changed, the

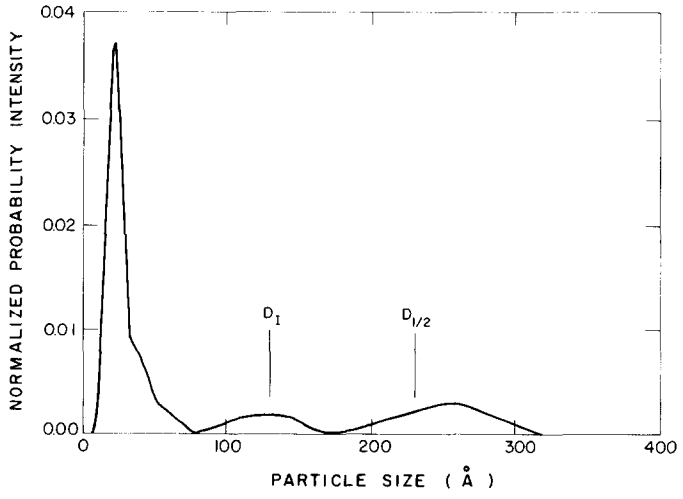

FIG. 2. Particle size distribution of catalysts prior to treatments at 600°C. The broad range in the particle size distribution is consistent with the large difference between $D_{1/2}$ and D_1, as shown. Also, note that the areas under all curves in this figure (and in subsequent PSD probability plots) are equal.

broad base of the line profile as seen on as-prepared samples (Fig. 1a) diminished steadily with increasing duration of the treatment. Such changes were clearly shown by the fact that the difference between $D_{1/2}$ and D_1 (Table 1) decreased steadily. For example, $D_{1/2}$ was found first to decrease from 230 to 180 Å after 16 h and then to increase to 210 Å after 64 h, while D_1 increased continuously from 130 to 170 Å. Overall, the ratios of $D_{1/2}$ to D_1 changed from ~1.8 for the as-prepared sample to ~1.2 after a 64-h treatment in O_2/N_2. A smaller difference between $D_{1/2}$ and D_1 indicates a PSD with a smaller variance. This was confirmed by the PSD analysis as described below.

PSD analysis (Fig. 3, curves 1 and 2) showed that, with continuous annealing of platinum catalysts in oxygen at 600°C, the small-particle peak showed a steady decrease in its intensity while shifting toward larger particle size from ~20 Å at $t = 0$ to ~40 Å at $t = 64$ h. Furthermore, the probability intensity within the particle size region immediately in front of the peak (~40 to 120 Å) increased more rapidly than that in other particle size regions (Fig. 3, curves 1 and 2). In contrast, the large-particle "peak," after first shifting slightly toward smaller particle size (16 h), remained almost unchanged in its position between 16- and 64-h treatments (Fig. 3, curves 1 and 2). The addition of CO_2 (a product of the reaction) to the mixture did not in any manner influence the progressive change in the PSD of the particles, nor did it affect the changes in D_1 or $D_{1/2}$ values (Table 1).

It was also noted that no platinum oxide phases were detected following the oxygen treatments. This suggests that if an oxide layer does exist it is very thin and will have no impact on the qualitative aspects of the results which are emphasized in this study. The fact that the strain was found to be insignificant also indicates that any surface oxygen has no effect on the platinum metal core. This observation is consistent with earlier work (*17*).

Sintering of platinum catalysts in prolonged treatments in wetted O_2 ($H_2O/O_2/N_2$; 2/6/92) and C_2H_4/N_2 (2/98) followed the same trend as that shown in oxygen treatments as described above (Table 1). That is, both wetted O_2 and C_2H_4 treatments produced PSDs with an increase in the probability intensity in the particle size region immediately next to the small-particle peak

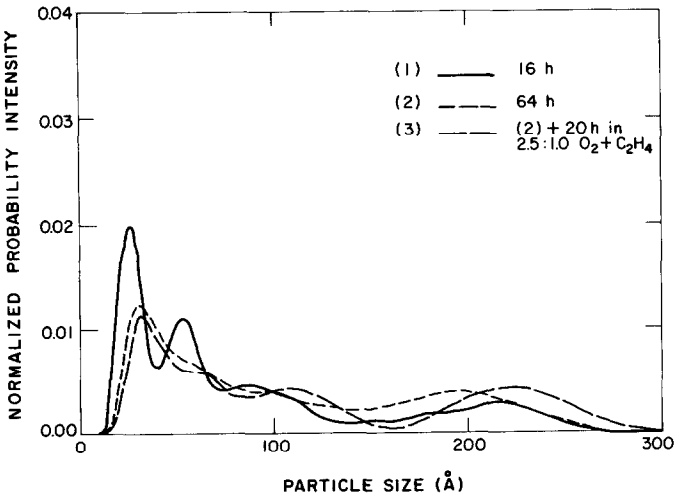

FIG. 3. Sintering in oxygen. Shown above are PSDs of catalyst samples following treatment at 600°C in (1) O_2/N_2 (6/94) for 16 h, (2) O_2/N_2 for 64 h, (3) O_2/N_2 for 64 h, plus 20 h in $C_2H_4/O_2/N_2$ (5/2/93).

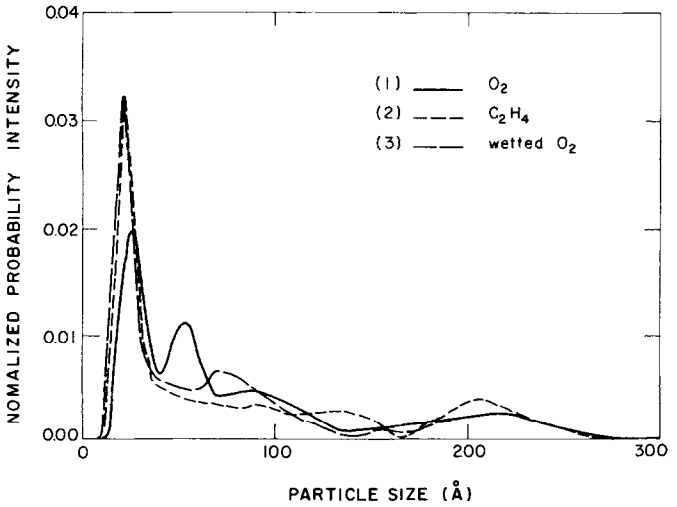

FIG. 4. Sintering in nonreactive atmospheres. Shown are PSDs of catalyst particles following treatments at 600°C in (1) O_2/N_2 (6/94) for 16 h, (2) C_2H_4/N_2 (2/98) for 16 h, (3) $H_2O/O_2/N_2$ (2/6/92) for 16 h.

and little long-term change in the position of the large-particle mode (Fig. 4). It must be noted that, just as in the case of oxygen treatment, initially there is a decrease in the average size of particles in the large-particle peak in both cases. However, it is also clear that the sintering of platinum is much slower in either wetted O_2 or C_2H_4 than in dry oxygen, as indicated by the higher intensity of the small-particle peaks in ethylene and wetted oxygen treatments (Fig. 4). The decrease in the sintering rate in the presence of water is also consistent with earlier microscope studies of Pt/SiO_2 model catalysts (*4*). Finally, it was also found that, following ethylene treatments, the catalysts became completely black indicating formation of carbon deposits due to the decomposition of ethylene.

Sintering during ethylene oxidation. Growth of platinum crystallites was also observed following prolonged treatment in the oxygen–ethylene mixtures at 600°C. However, the changes in the PSDs followed a trend different from those observed in the nonreactive gas treatments as described above. For example, the basic differences among their PSDs is that, after 64-h treatments under either fuel- (Fig. 5) or oxygen-excess (Fig. 6) conditions, the large-particle peak shifted toward larger particle size while there was only a slight change in both the intensity and the position of the small-particle peak. Meanwhile, in contrast to that in oxygen treatments, no significant increase in the intensity within the particle size region next to the small-particle peak was observed throughout the 64-h treatments. As a result, annealing under ethylene oxidation conditions produced particle size distributions with even larger variances than those in nonreactive gas treatments. Thus, it was not surprising to find that the X-ray line profiles of the catalysts treated in the oxygen–ethylene mixtures were similar to those of as-prepared samples (Fig. 1a) which showed a large departure from the Gaussian behavior. The rapid growth of the very large particles was also evident on the basis of a much larger increase in the $D_{1/2}$ values under the reaction conditions than in nonreactive gas treatments (see Table 1). It is interesting to note that there was no evident impact of running the reaction under fuel-excess as opposed to oxygen-excess conditions. This indicates that thermal gradients play no role in determining the nature of the sintering

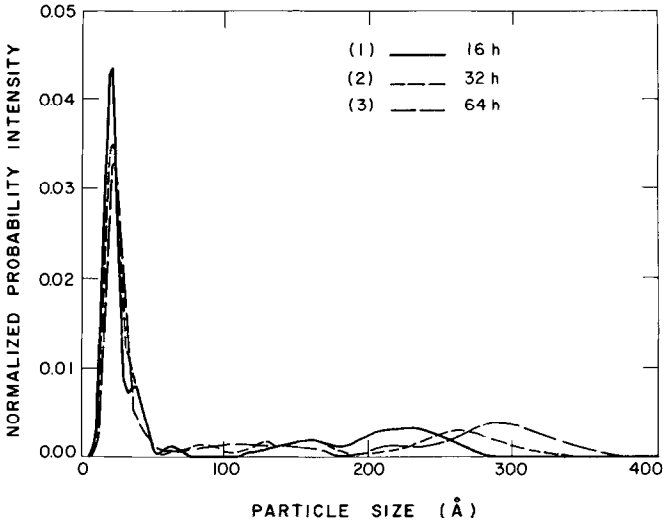

FIG. 5. Sintering under fuel-rich reaction conditions. Shown are PSDs of catalyst particles following treatments at 600°C in $C_2H_4/O_2/N_2$ (2/5/93) for (1) 16 h, (2) 32 h, (3) 64 h.

process as previous work (7) has suggested there are virtually no gradients under fuel-excess conditions and relatively large gradients under oxygen-excess conditions. The existence of temperature gradients could not be confirmed as discussed under Experimental.

In a separate experiment, a sample which had first been treated in O_2/N_2 for 64 h (Sample 0-3 in Table 1) was further treated in a fuel-rich $C_2H_4/O_2/N_2$ (2/5/93) mixture for 20 h (Sample 0-3a in Table 1). It was found that, while the position of the large-particle tail front of this sample remained unchanged in the final 48 h of O_2/N_2 treatment (Fig. 2, curves 1 and 2), it shifted dra-

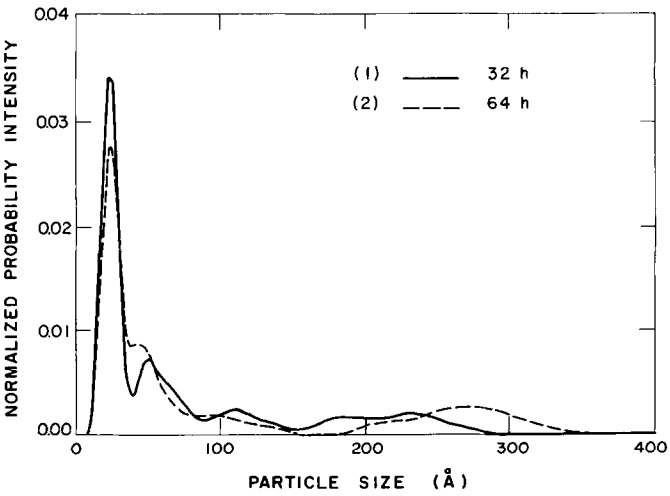

FIG. 6. Sintering under oxygen-rich reaction conditions. Shown are PSDs of catalyst particles following treatments at 600°C in $C_2H_4/O_2/N_2$ (2/8/90) for (1) 32 h, (2) 64 h.

matically toward the larger particle size after the treatment under the reaction conditions (Fig. 2, curve 3). This is also indicated by its large increase in $D_{1/2}$ as shown in Table 1.

DISCUSSION

Currently there are two sintering models. They are coalescence and intraparticulate atomic transport (*1, 2*). In brief, in the coalescence mechanism, metal particles are assumed to be mobile, moving along the surface of the support during high-temperature annealing. The sintering process proceeds via the coalescence (recrystallization) of colliding metal particles to form larger particles. In the intraparticulate atomic transport model, metal particles are assumed to be stationary, and the sintering results from the transport of metal atoms among the particles in such a way that the rate of loss of metal atoms is smaller than the rate of capture for large particles while the rate of loss is greater than the rate of capture for small particles. This results in the growth of larger particles at the expense of smaller particles.

A couple of simple criteria have been widely used in earlier sintering studies to distinguish between these two sintering mechanisms. For example, it has been proposed that the change in the particle size, and hence the metal surface area as a function of the duration of the heat treatment, will follow a simple power-law relationship, in which the order of such time dependence can be used to determine the sintering mechanisms (*23–25*). This simple criterion is considered unsatisfactory for this study for the following reasons. First, as shown under Results the value of the "average particle size," such as either $D_{1/2}$ or D_1, is sensitive to the methods used for the calculation. The time dependence calculated based on these different values will certainly follow different trends, allowing contradictory conclusions to be reached. For example, if the particle size calculated using the Debye–Sherrer equation, i.e., $D_{1/2}$, is used in this study to obtain a time-dependent relationship, the conclusion will be drawn that "redispersion" took place, i.e., the particles became smaller, following short periods (16 h) of treatments in all gas treatments (both nonreactive and reactive gas mixtures). However, in contrast, D_1, in all these cases, increases, steadily indicating a sintering process. Second, it is also clear that, for a catalyst with a broad PSD, no single number for "average particle size" can satisfactorily describe the sintering processes of a whole range of particle sizes. Moreover, recent theoretical studies (*26*) also show that the order of the power-law time dependence is sensitive to the width of the original PSDs, and thus it can actually vary over a wide range covering all the reported values even when the sintering process proceeds with the same sintering mechanism but with different initial PSDs.

The other simple criterion which has been widely used to determine the sintering mechanism is that coalescence will result in a long large-particle tail with decreasing probability intensity (*27, 28*), characteristic of a log-normal particle size distribution, while the intraparticulate atomic transport mechanism produces an almost mirror image PSD, i.e., a sharp peak at the very front of the large-particle side of the distribution (*23*). This criterion again does not hold because the initial PSD of the tested catalyst and the duration of the annealing can affect the final PSDs. This is clear from modeling studies. Figures 7 and 8 show results of computer modeling of sintering by coalescence and/or atomic migration. In neither figure do the distribution start or end with the "characteristic" shapes described above.

The computer simulation was conducted using a simplified version of the method proposed by Ruckenstein and Dadyburjor (*29*). The equations used are briefly described below. A more thorough discussion of this model can be found in the cited reference. The numerical calculation is carried out as follows. The rate of change of the

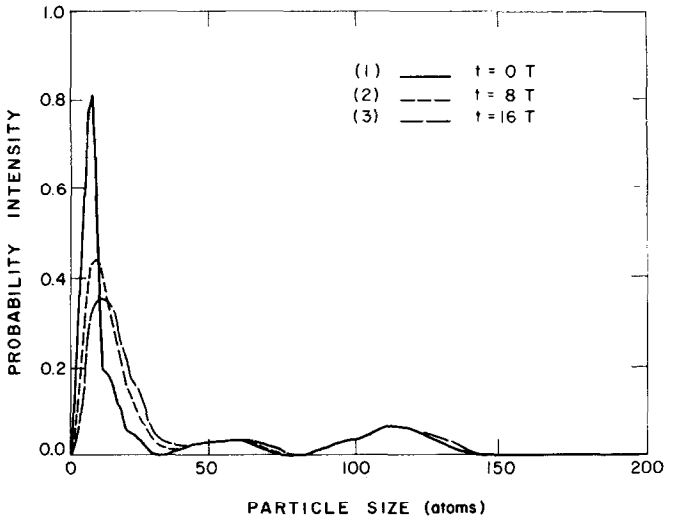

FIG. 7. Model of sintering via the coalescence mechanism. The model assumes that particles grow only by coalescence. Shown are (1) the initially assumed PSD, (2) PSD after 8 time units, (3) PSD after 16 time units.

number of particles of size j (contains j atoms) is given by

$$\frac{dn_j}{dt} = \alpha_{j+1}A_{j+1} + \beta_{j-1}n_{j-1} - \alpha_j n_j + \frac{1}{2}\sum_{i=2}^{j-2}\beta_{j-1,i}n_{j-1} - \sum_{i=2}^{\infty}(1 + \delta_{ij})\beta_{j,i}n_j \quad (1)$$

where α_j is the emission rate of single metal atoms from a particle of size j and $\beta_{j,i}$ is the capture rate of particles of size i by particles of size j. The equation is assumed to be valid only for aggregates of atoms ($j > 1$) and not for single atoms. The concentration of single atoms is calculated on the basis of

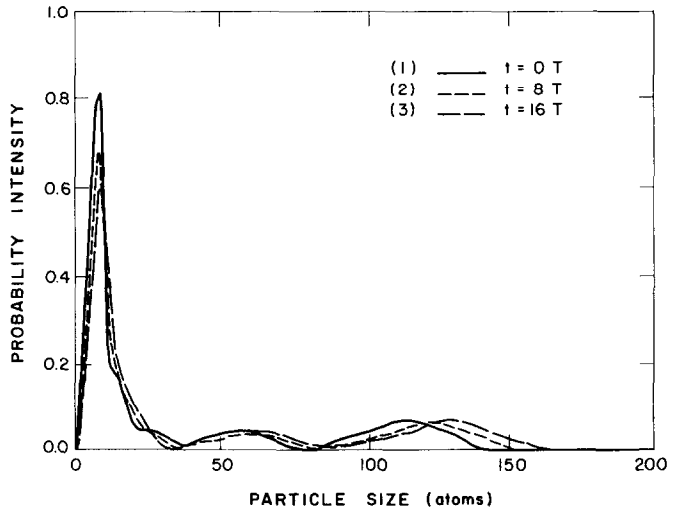

FIG. 8. Model of sintering via interparticle atomic transport. The model assumes that particles grow only by interparticle transport. Shown are (1) the initially assumed PSD, (2) the PSD after 8 time units, (3) the PSD after 16 time units.

mass conservation for the system as a whole.

The parameters of α and β are calculated as follows. In a manner analogous to the condensation relation, α_j is given by

$$\alpha_j = 2\pi r_j K_1 n_{1\infty}^{s} \exp\left[\frac{2\sigma V_m}{RTr_j}\right], \qquad (2)$$

where K_1 is the rate constant proportional to

$$\exp[-0.5(E_{mm} + E_{ms})/RT], \qquad (2a)$$

where E_{mm} is the metal–metal bond energy, E_{ms} the metal–substrate bond energy, r_j the radius of a j-atom particle assuming the particles are hemispherical, σ the interfacial free energy between metal and substrate per unit area, V_m the molar volume of the metal, and $n_{1\infty}^{s}$ the monomer concentration in equilibrium with an infinitely large crystallite.

The rate of capturing monomer, $\beta_{j,i}$, is calculated by

$$\beta_{j,i} = 2\pi r_j K_1' n_1, \qquad (3)$$

where K_1' is also proportional to $\exp[-0.5(E_{mm} + E_{ms})/RT]$ and n_1 is the bulk concentration of single atoms. For capturing particles containing more than two atoms the capture rate, $\beta_{j,i}$ ($i \geqq 2$), is approximated as

$$\beta_{j,i} \propto D_{j,i} n_j. \qquad (3a)$$

Assuming that diffusion is rate controlling during growth by coalescence (*2*), the capture rate $\beta_{j,i}$ is approximated as

$$\beta_{j,i} \propto D_{j,i} n_j, \qquad (4)$$

where $D_{j,i}$ is the diffusivity coefficient of an i-atom particle near a j-atom particle. Moreover, it is assumed that the mobility of metal particles is inversely proportional to the metal–substrate contact area:

$$\beta_{j,i} = D_0(r_i + r_j)\left(\frac{1}{r_j^2} + \frac{1}{r_i^2}\right) n_i. \qquad (5)$$

If it is assumed that sintering takes place only by interparticle atomic transport (Fig. 8) then D_0 (diffusivity constant) is set equal to zero. On the other hand, if it is assumed that sintering occurs by coalescence only, the emission rate of single atoms (all α) is set equal to zero (Fig. 7).

TABLE 2

Parameter	Equation	Value	Remark
$2\sigma V m/kT$	(2)	12 Å	
$K_1 n_{1\infty}^{s}$	(2)	$1 \cdot 10^{14}$ cm/(T)	(T) = 1 time unit. See Figs. 7–9
$K_1 = K_1'$	(3)	$6 \cdot 10^{9}$ cm^3/(CT)	
Temperature		600°C	
$D_{0(i=5)}$	(4)	$1.5 \cdot 10^{-13}$ cm^3/(T)	For five atom particle
Δt	(1)	1/60 (T)	

Note. The values above were selected to be "physically reasonable" on the basis of values obtained for the same constants in a real system (*29*).

The parameters used in the calculations are given in Table 2. It is noted that the values were chosen such that a significant change in the model PSDs could be observed after a reasonable period of "model time" had elapsed. A complete listing of the program is available (*30*).

Finally, it is assumed in the calculated sintering models (Figs. 7 and 8) that the initial shape of the particle size distribution is bimodal and that the relative intensities of each mode are similar to those of the starting catalysts used in this study. However, it must be emphasized that the model distribution is not the same as the experimental distribution and that the maximum particle size in the computer models is only 300 atoms, and not 300 Å. (It was not possible to model the true distribution because of the number of differential equations involved.) Changes in the model particle size distributions as a function of the mechanism of sintering, coalescence, atomic migration, or a combination of both, were studied. It is suggested that the results of these model studies qualitatively apply to changes which should be expected for the real distributions. No proof is offered.

As shown in Figs. 7 and 8, it is found that, in the case of sintering of catalysts with broad PSDs, the large-particle tail per-

sists for both mechanisms. In fact, the PSD which results from atomic transport is even broader than that resulting from coalescence. This is completely opposite to the standard criterion, indicating that this second criterion is also not applicable to the study of the sintering of catalysts with broad initial PSDs, and finite annealing periods.

From Figs. 7 and 8 it is also found that the basic difference between the PSD evolutions via the two different mechanisms resides in the extent of changes in the large-particle "peak" relative to the changes in the small-particle-size "peak." That is, in the case of the coalescence mechanism (Fig. 7) the decrease in the intensity of the small-particle mode is always associated with (i) a rapid intensity increase over the particle size region immediately in front of the peak and (ii) little change shown by the large-particle peak. In contrast, in the case of intraparticulate atomic transport (Fig. 8), there is a rapid shift in the large-particle peak toward larger particle size, only a small decrease in the intensity of the small-particle peak, and little change in the medium-particle-size region. These differences can be explained as follows. The growth of metal particles via the coalescence mechanism results primarily from the collision of moving particles. Thus, the fraction of the distribution with a large number of small particles will sinter more rapidly because the smaller the particle size, the higher the mobility. Mobility decreases rapidly with increasing size. Furthermore, it must be understood that the distributions reported in this work are volume distributions, and thus there are actually very few particles (relatively) which belong to the large-particle peak. In sum, the larger the relative number, and the smaller the size of the metal particles, the higher the probability they can collide and coalesce to form larger particles. This results in more coalescence processes involving particles in the small peak. In contrast, the intraparticulate atomic transport proceeds under a driving force such that the largest particle has the largest net influx of metal atoms. This results in a shift of the large-particle mode toward the larger particle size region, little change in the probability intensity over the medium-particle-size region, and a gradual decrease in the population of the smallest sized particles.

Based on the results of the modeling described above, it is proposed that the sintering of platinum catalyst under nonreactive gas treatments observed in this study proceeded primarily via the coalescence mechanism, while it is intraparticulate atomic transport that dominates under the reaction conditions used in this study. That is, it was repeatedly found during nonreactive gas treatments that the most significant change in the final PSD occurred in the particle size range next to the small-particle peak (Fig. 2). Qualitatively, this is the same change observed in the model of growth by coalescence (Fig. 7). Under reaction conditions it was found that the large-particle peak shifted forward, there was no increase in midsize particle numbers, and there was a gradual diminution in the number of small particles, without a concomitant change in the shape of that peak. Qualitatively, these are the same changes observed in the model of growth by atomic transport (Fig. 8). The qualitative agreement between growth by atomic transport with the types of changes observed following reaction treatments imposes another condition on a complete model of growth under reaction conditions. That is, it is necessary to explain why coalescence growth stops under reaction conditions. As shown in Fig. 9, the characteristics of changes in the PSD due to both coalescence and atomic transport acting concomitantly should be apparent in the shape of the final PSDs. This shape was not observed in the results reported. Finally, it must be noted that neither model explains the decrease in the average size of particles in the large-particle peak observed following all gas treatments of 16 h or less. This observation,

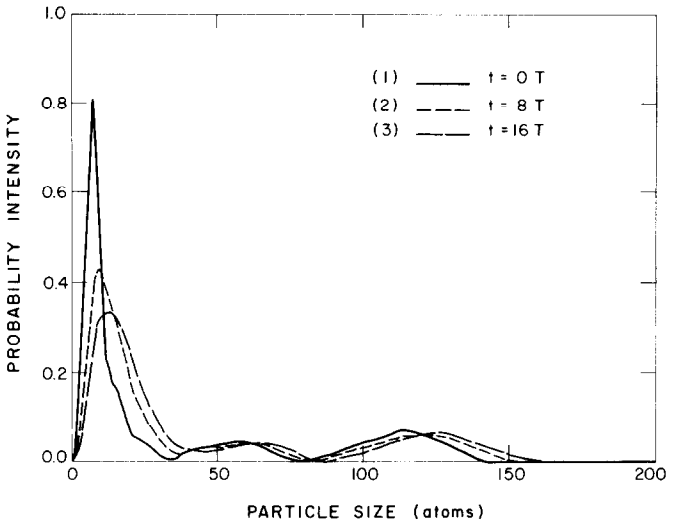

FIG. 9. Model of combined coalescence and interparticle atomic transport sintering. Both mechanisms are permitted to occur simultaneously in this model. Shown are (1) the initially assumed PSD, (2) the PSD after 8 time units, (3) the PSD after 16 time units.

consistent with earlier studies, requires another explanation as discussed later.

The increase in the platinum atom transport, which apparently takes place under reaction conditions, is consistent with the results of previous catalytic etching studies of platinum foils and thin films. As described elsewhere (*7, 8*) massive platinum migration takes place between approximately 500 and 700°C under ethylene oxidation conditions, under both fuel-excess and oxygen-excess conditions, resulting in dramatic surface reconstructions. The conditions used in this study fall exactly in the middle of this region. The unusual platinum atomic transport (which did not occur during etching in each single reactant (O_2, C_2H_4) and major reaction product (H_2O, CO_2) atmospheres over the same temperature range) was attributed to the interaction of gas-phase radicals, created during homogeneous reaction between oxygen and ethylene, and the platinum surface to form mobile, platinum-containing intermediates. Thus, the following model is proposed to explain the sintering of supported platinum catalysts at 600°C under ethylene oxidation: Homogeneously formed radicals interact with the supported platinum particles to form mobile, metastable intermediates. These mobile intermediates rapidly decompose upon interaction with any portion of the catalyst surface, leaving behind platinum atoms which migrate until they interact with and are adsorbed by a stable particle. The net result of this process is the movement of platinum between the particles in a manner very akin to that generally understood to take place during the atomic transport mechanism of sintering; there is a growth of large stationary particles at the expense of small stationary particles.

The final part of the model of growth under reaction conditions is that there is virtually no growth by coalescence. This can be justified on the basis of an empirical correlation with the sintering which occurs in wetted O_2 and C_2H_4 treatments (Fig. 3; Table 1). These results show that there is a decrease in the rate of coalescence sintering when either ethylene or water (even with oxygen) is present. Since previous etching studies show that recrystallization of polycrystalline platinum thin films in O_2, C_2H_4, and H_2O proceeds at the same rates (*7, 8*), it is suggested that the reduction in

the sintering rate of platinum catalysts in wetted O_2 and C_2H_4 is due to a decrease in the particle mobility, not to a slower recrystallization step following collisions between particles. Under reaction conditions water and/or carbon is also assumed to slow particle migration.

Finally, it was found following treatments in all nonreactive gas atmospheres that initially there is a decrease in the average size of particles in the large-particle peak of the distribution. It has been found by many workers that platinum particles redisperse following brief periods of oxygen treatment (e.g., 2 h) and sinter during longer treatments (*3, 5, 31–36*). This phenomenon is attributed by the majority of workers to the splitting of partially oxidized particles during the initial stages of treatment. It is generally reported to happen only to relatively large particles (*36*). It should also be pointed out that silica-supported platinum particles have been found to split at oxygen partial pressures on the order of 5×10^{-3} Pa which is about equal to the lowest "vacuum" pressure obtained in the present study (*37*). That study clearly showed that the oxygen partial pressure need not be high for particle splitting to take place.

There are alternative models (*33, 37*) to explain the initial regeneration of large particles. For example, Fiedorow and Wanke (*33*) suggest that particle growth is due to surface migration of PtO_2 species. They carefully exclude the possibility that it results from vapor-phase transport by PtO_2, as they correctly point out that even at 700°C the equilibrium vapor pressure of PtO_2 is so low that it cannot contribute significantly to metal transport. Indeed, a simple calculation (i) using the PtO_2 equilibrium vapor pressure formula of Alcock and Hooper (*38*); (ii) accounting for the fact (*39*) that the vapor pressure is directly proportional to the partial pressure of oxygen; (iii) assuming Pt particles of only 10% dispersion; and (iv) assuming an equilibrium vapor pressure of PtO_2 is maintained in all the flowing gas (unlikely, see Ref. (*40*)), it is found that it would take more than 100 years at 600°C to remove just the surface layer of the particles used in the present study. Furthermore, to explain why atomic migration via PtO_2 diffusion results in redispersion and not sintering, those workers postulated an increase in the total number of particles due to trapping of PtO_2 at strongly reacting sites on the alumina, and PtO_2/PtO_2 collisions leading to nucleation and growth of new particles. Both of those possibilities are excluded from consideration in the modeling done in this paper (number of particles constant or decreasing) as they are considered unlikely. For example, why not all the strongly reacting sites covered in the original production of the catalyst? Also, there is no evidence presented to show that the concentration and cross sections of migrating atomic species are large enough for significant interaction between these species to occur.

SUMMARY

Studies using XRD and computer modeling suggest that the sintering of silica-supported platinum catalysts under ethylene oxidation at 600°C, where massive platinum atomic transport was observed in previous etching studies, followed exclusively the intraparticulate atomic transport mechanism, while sintering in single reactant and heterogeneous reaction product species including O_2/N_2 (3/97), $H_2O/O_2/N_2$ (2/3/95), $CO_2/O_2/N_2$ (2/3/95), and C_2H_4/N_2 (2/98) followed primarily the coalescence mechanism. The increased atomic transport under the reaction conditions is consistent with the results of previous etching studies and can be readily explained by a model which postulates the formation of volatile platinum-containing intermediates via the interaction of gas-phase radicals and the platinum particles, and their subsequent decomposition elsewhere on the surface. Furthermore, reduction in the mobility of platinum particles under the reaction conditions was attributed to H_2O and/or carbon pres-

ent on the surface during the ethylene oxidation. This is consistent with the observations that sintering of platinum in $H_2O/O_2/N_2$ and in C_2H_4/N_2 is much slower than in O_2/N_2. Finally, it is clear that the "regeneration" behavior of large particles observed following short-term treatments is completely consistent with the results reported by many workers and is probably best explained by the particle splitting model.

REFERENCES

1. Wanke, S. E., and Flynn, P. C., *Catal. Rev. Sci. Eng.* **12,** 93 (1975).
2. Wynblatt, P., and Gjostein, N. A., *Prog. Solid State Chem.* **9,** 21 (1975).
3. Flynn, P. C., and Wanke, S. E., *J. Catal.* **37,** 432 (1975).
4. Chen, M., and Schmidt, L. D., *J. Catal.* **55,** 348 (1978).
5. Ruckenstein, E., and Chu, Y. F., *J. Catal.* **59,** 109 (1979).
6. Flytzani-Stephanopolous, M., and Schmidt, L. D., *Prog. Surf. Sci.* **9,** 83 (1979).
7. Wu, N. L., and Phillips, J., *J. Phys. Chem.* **89,** 591 (1985).
8. Wu, N. L., and Phillips, J., *J. Appl. Phys.* **59,** 769 (1986).
9. Wu, N. L., and Phillips, J., *Surf. Sci.* **184,** 463 (1987).
10. Ganesan, P., Kuo, H. K., Saavedra, A., and Angelis, R. J., *J. Catal.* **52,** 310 (1978).
11. Bertant, Par E. F., *Acta Crystallogr.* **3,** 14 (1950).
12. Mikkola, D. E., and Cohen, J. B., *in* "Load Atomic Arrangement Studied by X-Ray Diffraction" (J. B. Cohen and J. E. Hilliard, Eds.), p. 289. Gordon & Breach, New York, 1966.
13. Warren, B. E., and Averbach, B. L., *J. Appl. Phys.* **21,** 595 (1950).
14. Stokes, A. R., *Proc. Phys. Soc. London* **61,** 382 (1948).
15. Gangulee, A., *J. Appl. Crystallogr.* **7,** 434 (1974).
16. Mignet, J., and Rondont, D., *Acta. Metall.* **23,** 1321 (1975).
17. Sashital, S. R., Cohen, J. B., Burwell, R. J., Jr., and Butt, J. B., *J. Catal.* **50,** 479 (1977).
18. Pausescu, P., Manaila, R., Popescu, M., and Jijorici, E., *J. Appl. Crystallogr.* **7,** 281 (1974).
19. Renonprez, A., Hoang-Van, C., and Campagnon, P. A., *J. Catal.* **34,** 411 (1974).
20. Wu, N. L., and Phillips, J., unpublished data.
21. Smith, W. L., *J. Appl. Crystallogr.* **5,** 127 (1972).
22. Rothman, R. L., and Cohen, J. B., *Adv. X-Ray Anal.* **12,** 208 (1969).
23. Chakraverty, B. K., *J. Phys. Chem. Solids* **28,** 2401 (1967).
24. Wynblatt, P., and Ahn, T. M., *in* "Material Science Research" (G. C. Kuczynski, Ed.), Vol. 10, p. 83. Plenum, New York, 1975.
25. Ruckenstein, E. R., and Pulvermacher, B., *AIChE J.* **19,** 357 (1973).
26. Flynn, P. C., and Wanke, S. E., *J. Catal.* **34,** 390 (1974).
27. Granqvist, C. G., and Buhrmam, R. A., *J. Catal.* **42,** 477 (1976).
28. Granvqist, C. G., and Buhrmam, R. A., *J. Appl. Phys.* **47,** 2200 (1976).
29. Ruckenstein, E. R., and Dadyburjor, D. B., *J. Catal.* **48,** 73 (1977).
30. Wu, N. L., Ph.D. thesis, Pennsylvania State University, 1987.
31. Johnson, M. F. L., and Keith, C. D., *J. Phys. Chem.* **67,** 200 (1963).
32. Jaworska-Galas, Z., and Wrzyszcz, J., *Int. Chem. Eng.* **6,** 604 (1966).
33. Fiedorow, R. M., and Wanke, S. E., *J. Catal.* **43,** 34 (1976).
34. Ruckenstein, E. R., and Malhotra, M. L., *J. Catal.* **41,** 473 (1981).
35. Gollob, R., and Dadyburjor, D. B., *J. Catal.* **65,** 473 (1981).
36. Camber, R., and Romanowski, W., *J. Catal.* **105,** 213 (1987).
37. Stulga, J. E., Wynblatt, P., and Tien, J. K., *J. Catal.* **62,** 59 (1980).
38. Alcock, C. B., and Hooper, G. W., *Proc. R. Soc. London A* **254,** 551 (1960).
39. Norman, J. W., Staley, H. G., and Bell, W. E., *J. Phys. Chem.* **71,** 3686 (1967).
40. Krier, C. A., and Jaffee, R. I., *J. Less-Common Met.* **5,** 411 (1963).